



## Path Integral Monte Carlo

Bernard Bernu, David M. Ceperley

published in

*Quantum Simulations of Complex Many-Body Systems:  
From Theory to Algorithms*, Lecture Notes,  
J. Grotendorst, D. Marx, A. Muramatsu (Eds.),  
John von Neumann Institute for Computing, Jülich,  
NIC Series, Vol. **10**, ISBN 3-00-009057-6, pp. 51-61, 2002.

© 2002 by John von Neumann Institute for Computing

Permission to make digital or hard copies of portions of this work for personal or classroom use is granted provided that the copies are not made or distributed for profit or commercial advantage and that copies bear this notice and the full citation on the first page. To copy otherwise requires prior specific permission by the publisher mentioned above.

<http://www.fz-juelich.de/nic-series/volume10>



# Path Integral Monte Carlo

Bernard Bernu<sup>1</sup> and David M. Ceperley<sup>2</sup>

<sup>1</sup> Laboratoire de Physique Théorique des Liquides  
UMR 7600 of CNRS, Université Pierre et Marie Curie  
boite 121, 4 Place Jussieu, 75252 Paris, France  
*E-mail: bernu@lptl.jussieu.fr*

<sup>2</sup> Department of Physics and NCSA University of Illinois  
Urbana-Champaign, Urbana, IL 61801, USA  
*E-mail: ceperley@uiuc.edu*

In these notes, we present the basis of path integral techniques for indistinguishable and boson particles. The numerical evaluations of physical equilibrium properties needs an accurate action for the many body problem and an efficient algorithm to sample the paths.

## 1 Introduction

Feynman's path integral formulation of quantum mechanics has been proven to be very well suited to condensed boson systems, such as liquid or solid  $^4\text{He}$ , and fermion systems, such as liquid or solid  $^3\text{He}$  or a hydrogen plasma. Here we focus on problems than can be described by the following non-relativistic Hamiltonian:

$$\mathcal{H} = - \sum_{i=1}^N \lambda_i \nabla_i^2 + \sum_{i<j} v(|\mathbf{r}_i - \mathbf{r}_j|) \quad (1)$$

where  $N$  is the number of particles and  $\lambda_i = \hbar^2/2m_i$ . The pair potential is exactly known for hydrogen plasma ( $v(r) = Z_i Z_j e^2/r$ ) and also very well known for the interaction between helium atoms<sup>2</sup>. The same method applies for both the smoother but long range Coulomb potential and for the short range but strongly repulsive interaction between helium atoms.

These notes are taken from the most part from the review article<sup>1</sup> “*Path Integrals in theory of condensed helium*” published in *Rev. Mod. Phys.* **67** 280 (1995) where the reader can find many more details concerning path integral techniques as well as the physics of condensed helium 4. In these notes we give a minimum needed to start with path integral computations.

The second part of the notes is devoted to the exact mapping of the quantum problem to a classical one and general considerations on how path integrals are done. Because most interesting physical quantum systems deal with indistinguishable particles, the second part is about Bose systems.

## 2 Mapping of the Quantum to a Classical Problem

All static properties of quantum system in thermal equilibrium are obtained from the thermal density matrix. It can be defined in terms of the exact eigenvalues and eigenfunctions:

$$\rho = e^{-\beta\mathcal{H}} = \sum_i |\phi_i\rangle e^{-\beta E_i} \langle\phi_i|. \quad (2)$$

The equilibrium value of an operator  $\mathcal{O}$  is:

$$\langle\mathcal{O}\rangle = Z^{-1} \text{Tr}\rho\mathcal{O} = Z^{-1} \sum_i e^{-\beta E_i} \langle\phi_i|\mathcal{O}|\phi_i\rangle, \quad (3)$$

where  $Z$  is the partition function:

$$Z = \text{Tr}\rho = \sum_i e^{-\beta E_i}. \quad (4)$$

In the previous equations, the traces have been expressed in the eigenfunction basis. In the following we shall work exclusively in a position basis where particles are labeled. In such a basis, the density matrix elements are non-negative and can be interpreted as probabilities. The density matrix elements are thus defined as:

$$\rho(R, R'; \beta) \equiv \langle R| e^{-\beta\mathcal{H}} |R'\rangle = \sum_i \phi_i^*(R) e^{-\beta E_i} \phi_i(R'), \quad (5)$$

where  $R = (\mathbf{r}^{(1)}, \dots, \mathbf{r}^{(N)})$ , and  $\mathbf{r}^{(i)}$  is the position of the  $i$ th particle. In space dimension 3,  $\rho(R, R'; \beta)$  is, in general, a function of  $6N + 1$  variables. In position representation, Eqs. (3-4) become:

$$\begin{aligned} \langle\mathcal{O}\rangle &= Z^{-1} \int dR \langle R| \rho\mathcal{O} |R\rangle \\ &= Z^{-1} \int dR dR' \rho(R, R'; \beta) \langle R'|\mathcal{O}|R\rangle, \quad \text{with} \end{aligned} \quad (6)$$

$$Z = \int dR \rho(R, R; \beta), \quad (7)$$

where the identity  $\mathbf{1} = \int dR' |R'\rangle \langle R'|$  is introduced. From the definition of  $\rho(\beta)$  (Eq. 2), one derives the Bloch Equation:

$$-\frac{\partial\rho}{\partial\beta} = \mathcal{H}\rho \quad (8)$$

with the initial condition  $\rho(0) = \mathbf{1}$ , which reads  $\rho(R, R'; 0) = \delta(R - R')$  in the position representation.

### 2.1 Basis of Path Integral

The following equation is the basis of the path integral method:

$$\rho(\beta_1 + \beta_2) = e^{-(\beta_1 + \beta_2)\mathcal{H}} = e^{-\beta_1\mathcal{H}} e^{-\beta_2\mathcal{H}}, \quad (9)$$

and in position representation:

$$\langle R | \rho(\beta_1 + \beta_2) | R' \rangle = \int dR'' \langle R | e^{-\beta_1 \mathcal{H}} | R'' \rangle \langle R'' | e^{-\beta_2 \mathcal{H}} | R' \rangle, \quad (10)$$

$$\rho(R, R'; \beta_1 + \beta_2) = \int dR'' \rho(R, R''; \beta_1) \rho(R'', R'; \beta_2) \quad (11)$$

By repeating this process  $M$  times, one has:

$$e^{-\beta \mathcal{H}} = (e^{-\tau \mathcal{H}})^M \quad (12)$$

$$\begin{aligned} \rho(R_0, R_M; \beta) &= \int \dots \int dR_1 dR_2 \dots dR_{M-1} \rho(R_0, R_1; \tau) \\ &\quad \times \rho(R_1, R_2; \tau) \dots \rho(R_{M-1}, R_M; \tau), \end{aligned} \quad (13)$$

where  $\tau = \beta/M$  is called the time step. The succession of the points  $(R_0, R_1, \dots, R_M)$  is called a path. Note that Eq. (13) is exact for any  $M > 0$ . In the limit  $M \rightarrow \infty$ , the path becomes continuous, but its derivative will be discontinuous at almost all points on the path. Equation (13) is useful because we can find sufficiently accurate analytical approximations of the density matrix at small  $\tau$ .

In order to go further, we explicitly use the Hamiltonian. Let us suppose it is split in two pieces:

$$\mathcal{H} = T + V, \quad (14)$$

where  $T$  and  $V$  are the kinetic and potential operators which, in general, do not commute. The primitive approximation neglects all commutators between  $T$  and  $V$ :

$$e^{-\tau \mathcal{H}} \approx e^{-\tau T} e^{-\tau V}, \quad (15)$$

where the error is proportional to  $\tau^2$ . One can think that such approximation will lead to large error when the number of steps  $M$  increases ( $\tau = \beta/M \rightarrow 0$ ). But, the Trotter formula shows this is a well controlled process provided the operators are bounded below<sup>3</sup>:

$$e^{-\beta \mathcal{H}} = \lim_{M \rightarrow \infty} \left[ e^{-\frac{\beta}{M} T} e^{-\frac{\beta}{M} V} \right]^M. \quad (16)$$

We now write the primitive approximation Eq. (15) in the position representation:

$$\rho(R, R'; \tau) \approx \int dR'' \langle R | e^{-\tau T} | R'' \rangle \langle R'' | e^{-\tau V} | R' \rangle. \quad (17)$$

Usually the potential is diagonal in position representation:

$$\langle R'' | \exp(-\tau V) | R' \rangle = \exp(-\tau V(R')) \delta(R'' - R'). \quad (18)$$

The kinetic operator is diagonal in the reciprocal space. In a 3-dimensional box of length  $L$ , the free particle density matrix elements reads:

$$\begin{aligned} \rho_0(R, R'; \tau) &= \langle R | e^{-\tau T} | R' \rangle \\ &= \sum_{\mathbf{n}} L^{-3N} e^{-\tau \lambda 4\pi^2 \mathbf{n}^2 / L^2 - 2i\pi \mathbf{n} \cdot (R - R') / L} \\ &= \frac{1}{(4\pi \lambda \tau)^{3N/2}} \exp\left(-\frac{(R - R')^2}{4\lambda \tau}\right), \end{aligned} \quad (19)$$

where  $\mathbf{n}$  is a vector with integer components and the last equality holds when the “size” of a particle (its thermal wavelength) is much smaller than the size of the box<sup>4</sup>:

$$\tau\lambda \ll L^2. \quad (20)$$

Inserting these expressions (Eqs. 18-19) in the primitive approximation (Eq. 17) and using it in Eq. (13) gives:

$$\rho(R_0, R_M; \beta) = \int \dots \int dR_1 dR_2 \dots dR_{M-1} \frac{1}{(4\pi\lambda\tau)^{3NM/2}} \exp\left(-\sum_{m=1}^M \left[\frac{(R_{m-1} - R_m)^2}{4\lambda\tau} + \tau V(R_m)\right]\right). \quad (21)$$

Thus the density matrix can be calculated at any temperature from an integral over the paths  $R_1, \dots, R_{M-1}$ . Such an integral looks like a partition function of some classical system. In particular, we see here that the integrand is always non-negative and can be interpreted as a probability; an essential property for Monte Carlo simulations.

## 2.2 Classical Isomorphism

We have now all pieces to understand the classical isomorphism. Let us start with a single particle where  $V$  might be some external potential. The path consists of a list of points  $\mathbf{r}_0, \dots, \mathbf{r}_M$ . In Eq. (21), the first term in the exponential  $(\mathbf{r}_{m-1} - \mathbf{r}_m)^2/4\lambda\tau$  can be interpreted as the energy of a spring. Thus, a path is interpreted as a polymer where only first neighbors in the chain are connected with springs. Moving a quantum particle is equivalent to evolve this polymer<sup>6</sup>. If we have many free particles, using the identity

$$\sum_{m=1}^M (R_{m-1} - R_m)^2 = \sum_{m=1}^M \sum_{i=1}^N (\mathbf{r}_{m-1}^{(i)} - \mathbf{r}_m^{(i)})^2 = \sum_{i=1}^N \sum_{m=1}^M (\mathbf{r}_{m-1}^{(i)} - \mathbf{r}_m^{(i)})^2, \quad (22)$$

we see that each particle can be interpreted as a polymer with strings connecting nearest neighbors in each chain. Thus quantum particles are represented by polymers in Path Integral language. Now adding the potential interaction between particles does not change this picture (see Fig. 1). We only have interacting polymers. But these polymers are simpler than classical polymers as the potential interactions occur only at the same “time” in the path. Indeed, in Eq. (21), the potential term depends only on  $R_m$ , which means that only the beads of the paths at the same time ( $\tau m$ ) interact. In a real polymer, all beads interact with each other.

Most of the equilibrium quantities, such as energies, are obtained from the partition function (see Eq. (7)). In that case, the starting and ending beads of the polymers are the same:  $R_M \equiv R_0$  (see Fig. 2). Quantum particles are represented by ring polymers, and the paths expression is symmetric under a cyclic permutation of  $(R_0, \dots, R_{M-1})$ , thus any time can be chosen as a reference time. Note that this is true only for ring polymers. It is very instructive to keep in mind this picture that quantum particles are mapped on “classical polymers” with specific interactions.

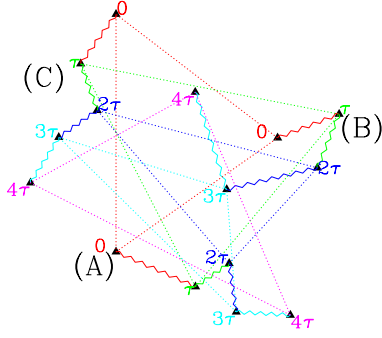


Figure 1. Cartoon of a path for 3 particles ( $A$ ,  $B$ ,  $C$ ) with  $M = 4$ ,  $\tau = \beta/4$ . The kinetic terms are represented by zig-zag lines and potential by dotted lines. Note that dotted lines connect only beads of the polymers at the same time

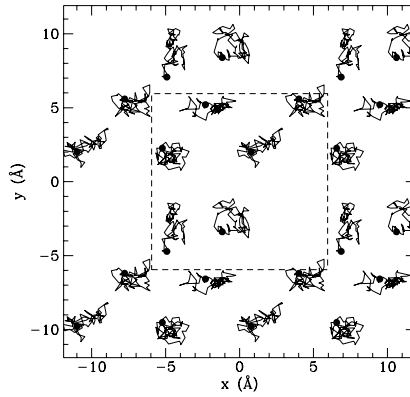


Figure 2. The trace of the close paths of six helium atoms at a temperature of  $2K$  with  $M = 80$ . Straight lines (kinetic term) connect successive beads of the polymers. The filled circles are markers for the (arbitrary) beginning of the path. The paths have been replicated using the periodic conditions. The dashed lines represent the simulation cell.

### 2.3 Definition of the Action

The action is defined as minus the logarithm of the density matrix. For a given link  $m$  (see Eq. 13), one has:

$$S_m \equiv S(R_{m-1}, R_m; \tau) \equiv -\ln[\rho(R_{m-1}, R_m; \tau)]. \quad (23)$$

Then, the exact path integral expression (Eq. 13) becomes:

$$\rho(R_0, R_M; \beta) = \int \dots \int dR_1 dR_2 \dots dR_{M-1} \exp\left(-\sum_{m=1}^M S_m\right). \quad (24)$$

The action has an exact kinetic (free particle) contribution denoted  $K_m$ :

$$K_m = \frac{3N}{2} \ln(4\pi\lambda\tau) + \frac{(R_{m-1} - R_m)^2}{4\lambda\tau} \quad (25)$$

All the rest of the action is the inter-action (potential) contribution:

$$U_m \equiv U(R_{m-1}, R_m; \tau) = S_m - K_m \quad (26)$$

The primitive approximation reads:

$$U_m \equiv \frac{\tau}{2} [V(R_{m-1}) + V(R_m)], \quad (27)$$

where Eq. (18) has been symmetrized, a property of the exact action<sup>5</sup>. Note this symmetrized form of the primitive action leaves unchanged Eq. (21) only for ring polymers where  $R_0 \equiv R_M$ .

With the primitive action one usually will need a large number of beads to get accurate properties, because this approximation is correct only at very small  $\tau$  (high temperature). Semi-classical expansions give expressions which are even more singular at short distances (as they involve derivatives of the potential which are usually singular at the origin). But, one can considerably reduce the number of beads by solving “exactly” all partial two body problems<sup>1</sup>. It is then possible to write an  $N$ -body action that will be good as long as three body collisions are negligible. For helium such a good action is obtained at  $\tau = 1/40K$ . See the review for how to get a “good” action.

## 2.4 Sampling the Path

Once, one has the “best” available action for the many-body system, one has to define the moves. Path Integral methods are usually used within the context of generalized Metropolis, or Markov chain Monte Carlo methods. Other contributions will consider the possibility of using Molecular Dynamics methods to sample path space, but such methods are not applicable when quantum statistics are important.

### 2.4.1 Displacement

The simplest move consists in a translation of the whole path of a given number of particles. Such a move will not change the relative positions of the beads inside each polymer. Therefore, it does not change the kinetic energy. But they do change the potential energy as they do with classical Monte Carlo, though without relaxation of the internal bead position the potential so computed will be biased. Displacement moves are efficient to evaluate the potential energy, especially in the weak coupling regime.



### 2.4.2 Multislice Moves

To change the kinetic energy, one has to move the relative positions of the beads inside the polymer. Moving only one bead is very inefficient because of the springs connecting a bead with its neighbors. Thus it is necessary to have moves that will change several adjacent time-slices of the polymer. In practice, one cuts a slice  $(r_{m+1}^{(i)} \dots r_{m+l-1}^{(i)})$  of the polymer, and samples a new path starting at  $r_m^{(i)}$  and finishing at  $r_{m+l}^{(i)}$ . Several algorithms may be used to reconstruct the path. One can start at one end and build a path constrained to reach the other end. One can also use the bisection algorithm which first samples the mid point and if it is accepted, it then sample the mid point of each link, and so on. The efficiency of each algorithm is problem dependent. For most simulations of dense systems the bisection algorithm has been successful. The choice of the number of slices  $l$  of the polymer which is moved may be fixed or even better may be chosen at random. Multislice moves change the center of mass of the polymer and a change in the potential energy also. One can think such moves are enough, but in practice, it is always better to allow as many types of moves as possible.

### 2.4.3 Acceptance Ratio

All kind of moves may be tried, but we do not want to waste computer time trying moves that will be always rejected. On the other hand, when all moves are always accepted, we might worry about really moving in the phase space. In classical Monte Carlo, the parameters of the moves are usually chosen to get acceptance ratio of roughly 1/2. For moves with no good *a priori* sampling distribution, an acceptance ratio of 1/2 is correct. But when we have a very good *a priori* sampling distribution, for example at very small  $\tau$ , the acceptance ratio gets naturally close to 1. It is of great importance to check the acceptance ratio for each type of moves. For example, in the bisection algorithm, we often have a poor sampling distribution at the first levels and the acceptance ratio is small, but when a path is eventually accepted, it has moved far away. Then the rest of the path gets better chance to succeed as the sampling action gets better (because it corresponds to smaller  $\tau$ ). In this algorithm, the time spent to evolve points with a poor action is much smaller than the time spent to evolve points with a good action.

## 3 Bose Symmetry

The Bose density matrix must be completely symmetric under any permutation of particle labels. It is also the solution of the Bloch equation (Eq. 8) with the symmetrized initial condition:

$$\rho_B(R, R'; 0) = \frac{1}{N!} \sum_{\mathcal{P}} \delta(R - \mathcal{P}R') \quad (28)$$

If  $\rho$  is solution for distinguishable particles, then the Bose density matrix is written in position representation:

$$\rho_B(R, R'; \beta) = \frac{1}{N!} \sum_{\mathcal{P}} \rho(R, \mathcal{P}R'; \beta) \quad (29)$$

The bad news is that we have now to evaluate  $N!$  terms and there is no efficient algorithm to calculate it explicitly; in mathematics it is called a “permanent.” The good news is that all terms are positive and therefore the sum can be sampled by Monte Carlo. One has an additional discrete variable  $\mathcal{P}$ , a variable in the permutation space of  $N!$  elements. Thus one has only to add another type of move to the list of Monte Carlo moves.

At high temperature, the identity permutation dominates, while at zero temperature, all permutations have equal an probability. In classical polymer language, the action of a cyclic permutation  $\mathcal{P}$  with cycle length  $n$ , consists in opening the ring polymers involved in this permutation and making a single polymer out of them<sup>7</sup> with  $nM$  beads. Typically only 2, 3 and 4-body ring permutations are tried (see the Appendix). They have the highest probability of success and are enough to walk through the permutation space, because all permutations can always be written as a product of pair permutations. The permutation sampled after  $p$  Monte Carlo steps is the product of all the accepted permutation moves since the beginning of the simulation.

Using the classical isomorphism, one can now see how the permutations allow new physics: when the temperature decreases, the particles are less and less localized (the number of beads increases), but two adjacent beads of a polymer are still constrained by the kinetic action which prevents the decrease of the kinetic energy. At low temperature, the ring-polymers try to be as elongated as possible. When two of them collide (which means some of the same-time-beads are close together), only a few beads are concerned. Then when the pair-permutation is tried, it is tried on these few beads: in both polymers, the slices at the same times are cut and new paths connecting polymer 1 to polymer 2 are built. If this move is been accepted, we are left with a ring-polymer with twice as much beads. The resulting polymer is more spread out so the kinetic energy has decreased. At high temperature, the number of beads is small and a polymer looks like a ball and the probability to have exchanging polymers is small. As the temperature decreases, the number of beads increases and the probability of alignment increases. First to appear are pair permutations. Longer cycles appear as the temperature is lowered.

By still decreasing the temperature, more and more polymers join to build longer ones. At some temperature, like in a percolation transition, a polymer of macroscopic size forms, connecting all portions of the systems. When this happens, there is a phase transition, and we have a fraction of the atoms in a superfluid phase. Properties of the transition can be calculated within PIMC. In a periodic system, the order parameter is measured by the winding number: the number of times a polymer wraps around the periodic boundary conditions. With a winding polymer, it is not possible to enclose the polymer completely in the simulation cell by only moving the center of the periodic box. This transition does not change much the local arrangement of particles and thus the pair correlation function changes very little around the transition.

## 4 Applications

We close the paper with a short list of applications for atomic and molecular problems that have been done using PIMC.

## 4.1 Boltzmanons

First, there are applications considering only the diffraction effects of quantum mechanics and not the effect of statistics. This is important when the thermal wave length associated with the particles is no longer negligible with respect to the mean spacing between them. Examples are systems of helium atoms or hydrogen molecules for  $T > 5K$ . These calculations are often quantum corrections to the classical results. Some examples are:

- Quantum effects on the kinetic energy of helium and heavier atoms<sup>8</sup>.
- Quantum effects on solids, melting or liquid-vapor transitions: *i*) the isotopic shift of the helium melting transition<sup>9</sup>, *ii*) Debye-Waller factor of solid helium<sup>10</sup>, *iii*) quantum effects on the critical point of helium<sup>11</sup>.
- Atoms and molecules on various surfaces: *i*) rotations of molecules on a surface<sup>12</sup>, *ii*) wetting transition of helium<sup>13</sup>.
- Quantum effects on excess volumes of liquid hydrogen and neon mixtures<sup>14</sup>.

## 4.2 Bosons

There are a number of calculations concerned with the superfluid transition of  ${}^4He$ <sup>1</sup>. Because  ${}^4He$  is one of the simplest bosonic system for experimentalists as well as for theoreticians, it has been studied also in inhomogeneous conditions:

- droplets: superfluidity in doped helium/hydrogen droplets<sup>15</sup>
- hydrogen molecules can also Bose condensed and have been studied on surfaces, in mixture with helium and in confined geometry. For a review of bosons in surfaces geometry see ref.<sup>17</sup>.

The hard sphere model is useful for the new Bose-Einstein condensation<sup>16</sup>, for helium in porous media<sup>18</sup> and vortices in High- $T_c$  map onto bosons<sup>19</sup>.

## Appendix

### Permutation Sampling

In this section we describe the heat-bath algorithm to choose the permutation to be tried. The heat-bath probability for a permutation change between times  $i$  and  $i + m$  is:

$$T^*(\mathcal{P}) \propto \rho(R_i, \mathcal{P}R_{i+m}) \quad (30)$$

Within the end-point approximation, these density matrix elements have the same potential part (thus can be dropped out) and  $T^*$  depends only on the kinetic part:

$$T^*(\mathcal{P}) = \frac{1}{C_I} \exp \left[ - \sum_{j=1}^n \left( \mathbf{r}_i^{(j)} - \mathbf{r}_{i+m}^{(\mathcal{P}j)} \right)^2 / (4\lambda^* m\tau) \right], \quad (31)$$

where  $C_I$  is a normalization factor,  $\lambda^*$  is an effective mass to account off-diagonal contributions.  $T^*(\mathcal{P})$  (Eq. 31) can be computed from the square matrix of the distances between end points:

$$t_{kj} = \exp \left[ - \left( \mathbf{r}_i^{(k)} - \mathbf{r}_{i+m}^{(j)} \right)^2 / (4\lambda^* m \tau) \right]. \quad (32)$$

A random walk through this table will try to make a permutation of  $l$  atoms: the first atoms  $k_1$  is chosen at random, the second atom  $k_2$  is selected according to the probability  $t_{k_1, k_2} / h_{k_1}$  where  $h_{k_1} = \sum_k t_{k_1, k}$ . After all of the  $l$  labels are selected and it is verified that they are unique, the trial permutation is accepted with the probability:

$$A = \min \left[ 1, \frac{\sum_{i=1}^l h_{k_i} / t_{k_i, k_i}}{\sum_{i=1}^l h_{k_i} / t_{k_i, k_{i+1}}} \right], \quad (33)$$

where  $k_{l+1} \equiv k_1$ . The sum of terms comes from the various starting point of the cyclic permutation. The probability of acceptance is rare because the last link  $t_{k_l, k_1}$  has  $1/N$  chance to be not small (i.e. when the cycle closes on itself). But the process of constructing each loop is very rapid.

The physics help to fix the parameter  $l$ . On dense liquid, it is much to permute 3 or 4 than 2 atoms. A Monte Carlo simulation starts with the identity permutation. It is thus difficult to get pair exchanges accepted. On the contrary, once three and quadruple exchanges have build long cycles, pair exchanges can efficiently add or subtract from them. Also to get winding number changes, the parameter  $l$  must be large enough so that the permutation change can span the whole box.

## References

1. David Ceperley, *Rev. Mod. Phys.* **67** 280 (1995).
2. R.A. Aziz, M.J. Slaman, A. Koide, A.R. Allnatt, and W.J. Meath, *Mol. Phys.* **77** 321 (1992).
3. B. Simon, *Functional Integration and Quantum Physics*, (1979) Academic, New-York.
4. The volume of the box is proportional to the number of particles (at fixed density). Thus for large enough number of particles the condition of Eq. (20) is satisfied.
5. The density matrix is symmetric by the exchange of the end points. Thus any "good" approximation should have this property. Also if we expand Eq. (15) in power of  $\tau$ , the symmetrized form  $\exp(-\tau\mathcal{H}) \approx \exp(-\frac{\tau}{2}\mathcal{V}) \exp(-\tau\mathcal{T}) \exp(-\frac{\tau}{2}\mathcal{V})$  is correct to order 2 instead of order 1 for Eq. (15). Note also that this symmetrized form leaves unchanged the Trotter formula.
6. See for example the moves of a single particle in a harmonic well: <http://www.physics.buffalo.edu/phy411-506/lectures.html>
7. Note that only Monte Carlo techniques allow such type of moves, where the polymers often cross each other.
8. Ceperley, D. M., R. O. Simmons and R. C. Blasdel, *Phys. Rev. Lett.* **77** 115 (1996).
9. Boninsegni, M., Pierleoni, C. and Ceperley, D. M., *Phys. Rev. Lett.* **72** 1854 (1994); J.L. Barat, P. Loubeyre, M.L. Klein, *J. Chem. Phys.* **90** 5644 (1989); C. Chakravarty and R. M. Lynden-Bell, *Journal of Chemical Physics* **113** 9239(2000).

10. M. Neumann, M. Zoppi, *Phys. Rev. B* **62** 41 (2000); Draeger, E. W., and D. M. Ceperley, *Phys. Rev. B* **61** 12094 (2000).
11. M. Müser, E. Luijten, cond-mat/0105283.
12. D. Marks, M. Müser, *J. Phys. CM*, **11** R 117 (1999). T Cui, E Cheng, B J Alder, *Phys. Rev. B* **55** 12253 (1997).
13. M. Boninsegni and M.W. Cole, *J. Low Temp. Phys.* **110** 685 (1998).
14. S. R. Challa and J. K. Johnson, *J. Chem. Phys.* **111** 724 (1999).
15. Yongkyung Kwon, K. Birgitta Whaley, *J. Chem. Phys.* **115** 10146 (2001); *J. Chem. Phys.* **114** 3163 (2001).
16. Gruter, P., D. Ceperley and F. Laloe, *Phys. Rev. Lett.* **79** 3549 (1997).
17. D. Ceperley and E. Manousakis, to appear in *J. Chem. Phys.* (2001).
18. M. C. Gordillo and D. M. Ceperley, *Phys. Rev. Lett.* **85** 4735 (2000).
19. Sen, P., N. Trivedi and D. M. Ceperley, *Phys. Rev. Lett.* **86** 4092 (2001).